# Disturbed Cortico-Subcortical Interactions During Motor Task Switching in Traumatic Brain Injury

Inge Leunissen,[1] James P. Coxon,[1] Monique Geurts,[1]
Karen Caeyenberghs,[1] Karla Michiels,[2] Stefan Sunaert,[3]
and Stephan P. Swinnen[1]*

[1]Motor Control Laboratory, Research Centre of Movement Control and Neuroplasticity,
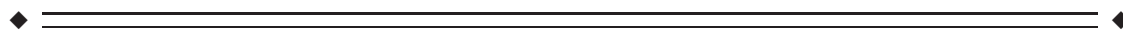Department of Biomedical Kinesiology, Group Biomedical Sciences, K.U. Leuven, Belgium
[2]Department of Physical Medicine and Rehabilitation, University Hospital,
Leuven Campus Pellenberg, Belgium
[3]Department of Radiology, University Hospital, K.U. Leuven, Belgium

◆ ━━━ ◆
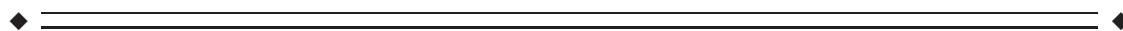
Abstract: The ability to suppress and flexibly adapt motor behavior is a fundamental mechanism of cognitive control, which is impaired in traumatic brain injury (TBI). Here, we used a combination of functional magnetic resonance imaging and diffusion weighted imaging tractography to study changes in brain function and structure associated with motor switching performance in TBI. Twenty-three young adults with moderate-severe TBI and twenty-six healthy controls made spatially and temporally coupled bimanual circular movements. A visual cue signaled the right hand to switch or continue its circling direction. The time to initiate the switch (switch response time) was longer and more variable in the TBI group and TBI patients exhibited a higher incidence of complete contralateral (left hand) movement disruptions. Both groups activated the basal ganglia and a previously described network for task-set implementation, including the supplementary motor complex and bilateral inferior frontal cortex (IFC). Relative to controls, patients had significantly increased activation in the presupplementary motor area (preSMA) and left IFC, and showed underactivation of the subthalamic nucleus (STN) region. This altered functional engagement was related to the white matter microstructural properties of the tracts connecting preSMA, IFC, and STN. Both functional activity in preSMA, IFC, and STN, and the integrity of the connections between them were associated with behavioral performance across patients and controls. We suggest that damage to these key pathways within the motor switching network because of TBI, shifts the patients toward the lower end of the existing structure-function-behavior spectrum. *Hum Brain Mapp 34:1254–1271, 2013.* © 2012 Wiley Periodicals, Inc.

Key words: bimanual coordination; cognitive control; fMRI; task switching; traumatic brain injury

◆ ━━━ ◆

INTRODUCTION

Traumatic brain injury (TBI) is a leading cause of death and disability in young adults [Kraus and McArthur, 1996; Sosin et al., 1996]. In the United States, ~2 million brain injuries occur each year, resulting in 56,000 deaths and 18,000 survivors with long-term physical, motor, cognitive, and emotional impairments [Colantonio et al., 2004; Sosin et al., 1996]. In Europe, epidemiological data on TBI is scare, but an incidence rate of about 235 per 100,000 and an average mortality of about 15 per 100,000 were derived [Tagliaferri et al., 2006] (For more information see Burns and Hauser [2003] and Maas et al., [2008]). The frontal and temporal lobes are particularly susceptible to traumatic brain damage with focal lesions generally occurring directly beneath the site of impact (coup injury), and sometimes opposite the impact as well (contre-coup injury). The impact also causes movement of the brain relative to the skull, resulting in widespread tearing and shearing (diffuse axonal injury, DAI) of white matter connections between the frontal cortex and related circuitry, such as the basal ganglia (BG), thalamus and cerebellum [Gentry et al., 1988; McDonald et al., 2002].

Behavioral work has shown that TBI patients are commonly impaired on working memory, executive function, attention, and processing speed tasks [Draper and Ponsford, 2008; Kraus and McArthur, 1996; Levin and Kraus, 1994; Scheid et al., 2006]. Functional magnetic resonance imaging (fMRI) studies investigating these domains show that TBI patients have increased and/or more broadly dispersed activity in frontal (NB: dorsolateral prefrontal cortex, DLPFC; anterior cingulate cortex, ACC) and parietal regions [Kim et al., 2009; Newsome et al., 2008; Scheibel et al., 2007; Turner and Levine, 2008].

Turner et al. [2011] showed that areas within PFC, normally coactivated during working memory, are behaviorally relevant at an earlier stage of difficulty for TBI patients as compared to controls. Patients did not recruit extra areas that were not engaged in the control sample, however, providing evidence for altered functional engagement in TBI as opposed to functional reorganization. Moreover, a widespread reduction of fractional anisotropy (FA), a measure of white matter microstructural integrity, is linked to worse performance on global measures of memory, executive function, and attention in TBI [Kinnunen et al., 2011]. Taken together, these studies suggest functional compensation may serve to minimize the effects of structural disruption on TBI patients' behavior. However, to date this has not been examined in the same group of patients.

TBI patients not only exhibit deficits in working memory and attention, but also in their ability to cognitively control their actions. This is particularly evident in situations where response conflict is high, and when inappropriate prepotent response tendencies have to be overcome [Larson et al., 2006; Levin et al., 2004; Mecklinger et al., 1999; Perlstein et al., 2006; Seignourel et al., 2005]. A few func-

tional imaging studies have investigated the resolution of interference in the presence of irrelevant stimuli by means of the Stroop task [Mani et al., 2007; Soeda et al., 2005; Tlustos et al., 2011]. These studies give insight into how the ability to ignore distracting information is affected in TBI. However, the neural mechanisms underlying the impaired ability to suppress inappropriate actions, or switch between them, remain unclear.

Accumulating evidence suggests that behavioral switching is mediated by interactions between the presupplementary motor area (preSMA) and BG nuclei [Hikosaka and Isoda, 2010; Mink, 1996; Nachev et al., 2008; Nambu et al., 2002; Rushworth et al., 2004]. The preSMA and SMA-proper are thought to be responsible for linking situations with appropriate actions [Nachev et al., 2008], and their input to the BG influences action selection via pathways, which serve to focus thalamocortical output [Hikosaka and Isoda, 2010; Mink, 1996]. The preSMA plays a critical role when a subject tries to stop an impending movement and when two procedures compete with each other [Aron and Poldrack, 2006; Coxon et al., 2010; Isoda and Hikosaka, 2007; Nachev et al., 2008; Rushworth et al., 2004]. There are monosynaptic "hyperdirect" projections to the STN from cortical structures, including preSMA and inferior frontal cortex (IFC) [Aravamuthan et al., 2007; Aron et al., 2007; Inase et al., 1999; Nambu et al., 2002], making STN a key node in the network for inhibitory control of action [Aron and Poldrack, 2006]. As the same network involving IFC, preSMA, and the BG supports both response inhibition and switching [Kenner et al., 2010], with inhibition considered a constituent process of switching [Monsell, 2003], we focused our analysis on this network using a combination of fMRI and DTI to study the neural basis of motor task switching in TBI.

Task switching was investigated in the context of ongoing bimanual coordination dynamics [Kelso and Fuchs, 1995] with subjects continuously drawing bimanual circles. Upon presentation of a cue, subjects switched between coordination patterns by changing direction with only the right hand. The literature on rhythmic bimanual coordination has established that asymmetric patterns [e.g., when both hands make counter clockwise (CCW) or clockwise (CW) circular motions] are less stable and more difficult to perform than symmetric patterns, during which the hands mirror each other with respect to the body midline (for review see [Swinnen, 2002]). Furthermore, behavioral studies show that intentional switching from the easier symmetric to the more difficult asymmetric movement pattern takes longer than vice versa, and switching via the dominant right hand frequently disrupts nondominant hand movement [Byblow et al., 1999, 2000; Coxon et al., 2010; Wenderoth et al., 2009]. Put differently, this form of switching temporarily dissociates the limbs from sharing an ongoing movement plan, requiring inhibition of a part of the existing plan [Coxon et al., 2010; Wenderoth et al., 2009].

We selected a large sample ($N = 23$) of chronic (>20 months) patients with moderate-severe TBI. Due to diffuse

injuries in the frontal lobe, thalamus and BG, disturbing the SMA-BG loop, we expected TBI patients to have difficulties performing the motor switching task. At the behavioral level, we predicted that TBI patients would take longer to implement pattern change via the right hand than the control subjects and that switching to asymmetric coordination would be more difficult than vice versa, with more contralateral disruptions of the non-dominant left hand in the TBI patients. These predictions were based on previous studies of reaction time and cognitive task switching in TBI [Larson et al., 2006; Schroeter et al., 2007] and previous work by our group, describing motor switching performance in an elderly population [Coxon et al., 2010]. Elderly and TBI patients share some degree of similarity with respect to changes in grey and white matter structure, such as atrophy and a reduction in white matter integrity, albeit for different reasons. Since structure constrains function and impacts upon behavior, we used the elderly as a model, predicting similar behavior in the TBI population. At the neuronal level, we hypothesized that TBI patients would show compensatory recruitment in cortical regions that support motor switching, such as preSMA, compared to healthy controls. Secondly, we expected the activity in these areas to covary with proficiency in switching. With respect to the DTI results, we expected widespread changes in white matter microstructural properties in TBI patients, reflected by reduced FA [Kinnunen et al., 2011]. Finally, we hypothesized that structural connection integrity would correlate with switching performance and functional activation, reflecting a tight linkage between brain structure, function, and behavior.

MATERIALS AND METHODS

Participants

Twenty-three young adults with TBI (mean age 24.5; range 16–34; 15 male) and twenty-six healthy volunteers (mean age 25.3; range 21–35; 11 male), were recruited. The groups did not differ significantly with respect to age ($t(47) = 0.94$; $P = 0.35$) or gender (Chi^2 = 2.57; $P = 0.11$). The demographic and clinical characteristics of the TBI group are shown in Table I. All TBI patients were assessed at least 6 months post-injury, when their neurological status had stabilized and they no longer participated in formalized rehabilitation or training programs. The time since injury was on average 4.8 yr (range 1–10; SD 2.8) and their age at injury was on average 19.6 yr (range 8–29; SD 5.9). According to the Mayo Classification System for TBI Severity, which relates to the duration of loss of consciousness, length of post-traumatic amnesia, lowest recorded Glasgow Coma Scale in the first 24 h, and/or CT or MRI images [Malec et al., 2007] assessed by our neuroradiologist (S.S.), our TBI group consisted of one mild case and 22 moderate-severe cases. Patients performed worse on clinical measures of bimanual coordination relative to controls, with less pegs inserted for the bimanual condi-

tion of the Purdue Pegboard Test ($t(41) = 3.94$, $P < 0.001$; controls: 13 ± 1.14 pegs; TBI patients: 11 ± 1.78 pegs), and a longer time to complete TEMPA bimanual tasks ($t(41) = -5.56$, $P < 0.001$; controls: 9.88 ± 1.39 sec; TBI patients: 13.03 ± 2.17 sec). Measures of cognitive function were also worse, Trail making A ($t(41) = -2.96$; $P < 0.01$; controls: 32.10 ± 7.26 sec; TBI patients: 40.50 ± 10.27 sec) and Trail making B ($t(41) = -2.02$, $P < 0.05$; controls: 61.69 ± 15.75 sec; TBI patients: 74.72 ± 24.78 sec). In contrast, hand strength did not differ between groups for either hand as determined by the JAMAR (left hand: $t(41) = 0.16$; $P = 0.87$; controls: 38.23 ± 13.32 lbs; TBI patients: 39.09 ± 8.08 lbs; right hand: $t(41) = -0.25$, $P = 0.80$; controls: 42.03 ± 14.87 lbs; TBI patients: 41.41 ± 10.13 lbs). For more detailed information see Supporting Information and Supporting Information Table I.

All participants were right-handed (laterality quotient: TBI: mean 81.5; Controls: mean 93.7) as verified by the Edinburgh Handedness Inventory [Oldfield, 1971]. For the DTI analyses, we included 18 TBI subjects and 18 healthy controls due to technical problems during DTI acquisition. For the TBI group, the three subjects with the largest focal lesions were excluded from the analyses (image artifacts or excessive head movements). The study was approved by the local ethics committee, and written informed consent was obtained prior to the experiment. Subjects over 18 signed the consent form themselves whereas a parent/caregiver signed the form for those under 18.

Imaging Protocol

Behavioral task

We used a protocol that has been used in a previous fMRI study in young and elderly healthy subjects [Coxon et al., 2010]. Participants were required to make spatially and temporally coupled circular motions with joysticks. For each hand, the direction of circling could be either CW or CCW. An auditory metronome was used for pacing such that participants completed one circle per tone. Four possible bimanual movement patterns were introduced: Inward circles (left hand CW, right hand CCW), outward circles (left hand CCW, right hand CW), CW circles (both hands CW), and counter-clockwise circles (both hands CCW). Inward and outward circling are symmetric bimanual movements, and CW/CCW circling are asymmetric with respect to the body midline. A constant visual display was shown comprising two white circles, each with a curved white bar immediately above, and a central fixation cross on a black background. Instruction cues were conveyed by arrows, visible for 800 ms (Fig. 1A). Green arrows were used as imperative cues. The initial pattern to adopt was indicated by two green arrows. A single green arrow pointing opposite to the actual movement direction indicated that the right hand must change direction (Switch). This resulted in a change of movement pattern from asymmetric to symmetric circling (SW»SYMM, easy switch) or from symmetric to asymmetric circling

TABLE I. Summary of demographic and injury characteristics for the TBI group

TBI patient #	Gender	Age (y)	Age at injury (y)	Time since injury (y)	Cause of injury	MRI scan at examination Lesion location/pathology	Focal lesion
TBI 1	F	17	12	5.1	Traffic accident	None	
TBI 2	F	16	8	7.9	Traffic accident	None	
TBI 3	F	22	21	1.6	Traffic accident	Hemosiderin deposits (R) PL and (R) FL	
TBI 4	F	26	23	3.0	Traffic accident	PL and OL/PL and FL and (R) TL shearing injuries, slightly enlarged ventricles	
TBI 5	M	22	17	4.8	Traffic accident	(R) FL contusion	
TBI 6	M	34	28	5.6	Traffic accident	(L) TL contusion	
TBI 7	M	16	9	7.8	Traffic accident	FL contusion, enlarged ventricles	
TBI 8	M	27	18	9.8	Traffic accident	Hemosiderin deposits thalamus and (L) OL	
TBI 9	M	28	18	9.5	Traffic accident	FL contusion	X
TBI 10	M	31	29	2.1	Traffic accident	TL and (R) FL contusion, (L) PL shearing injury, corpus callosum degeneration, asymmetric ventricles,	X
TBI 11	M	16	14	2.2	Fall	(L) corpus callosum and thalamus and (R) PL and (L) FL and (R) TL shearing injuries, right ventricle enlarged	
TBI 12	M	24	21	2.2	Traffic accident	FL and (L) cerebellum contusion	X
TBI 13	F	27	25	2.3	Traffic accident	(L) FL and TL contusion	
TBI 14	F	20	18	2.5	Traffic accident	FL and (R) PL contusion, FL shearing injuries, enlarged ventricles	X
TBI 15	M	30	28	2.6	Traffic accident	(L) TL contusion, (L) ACC and (R) FL and central sulcus shearing injuries	X
TBI 16	M	27	24	3.0	Traffic accident	Thalamus and corpus callosum and TL shearing injuries	
TBI 17	M	22	19	3.2	Traffic accident	(L) thalamus and (L) TL and FL and central sulcus shearing injuries	
TBI 18	F	19	15	3.4	Traffic accident	(L) PL contusion, corpus callosum and OL shearing injuries, left ventricle enlarged	X
TBI 19	M	28	18	9.7	Traffic accident	(R) FL and thalamus shearing injuries, corpus callosum degeneration	
TBI 20	M	33	27	6.0	Traffic accident	FL / OL contusion, thalamus and corpus callosum injuries	
TBI 21	M	27	20	6.2	Traffic accident	FL and (R) OL/PL contusion, corpus callosum degeneration	X
TBI 22	M	21	15	6.7	Traffic accident	FL contusion, (R) FL and (R) OL shearing injuries	X
TBI 23	M	30	23	6.8	Traffic accident	(L) TL and FL contusion, thalamus injury	X

Anatomy codes: FL, frontal lobe; TL, temporal lobe; PL, parietal lobe; OL, occipital lobe; ACC, anterior cingulate cortex; R, right; L, left.
Other codes: TBI, traumatic brain injury; MRI, magnetic resonance imaging; M, male; F, female.

(SW»ASYMM, hard switch). A single green arrow pointing in the same direction as the actual movement indicated that no change was necessary for the right hand (Continue). In both cases, the left hand was to maintain moving

in the already established direction. Four seconds after the imperative cue (in both switch and continue trials) white arrows indicated the correct movement. For participants, this served as confirmation that they were performing the correct pattern or provided an opportunity to correct their error.

Experimental procedure

Prior to the experiment, participants received a description of the task and their maximum stable movement frequency was determined. Participants lay in a dummy scanner, with their forearms supported at ∼45° from the horizontal, making circular motions about the wrist and metacarpophalangeal joints with their left and right index fingers by means of two custom joysticks (Fig. 1A). They were cued to move in an asymmetric pattern (both hands CW and CCW), and metronome frequency was increased every 8 s from 1 to 3 Hz in 0.25 Hz increments. The participant's maximum stable movement frequency was determined by online inspection of the relative tangential angle [Carson et al., 1997]. When either a spontaneous transition occurred or the temporal relationship to the metronome could no longer be maintained, the maximum stable frequency was recorded. During training and scanning sessions (see below), participants were paced at 50% of their maximum. This procedure served to establish common relative speeds, equating the difficulty of bimanual circling between groups. After establishing the maximum movement frequency, participants stayed in the dummy scanner for a training session to ensure that each subject could perform the task proficiently.

During the fMRI experiment, subjects performed five scanning runs, each 351 s in duration. A run comprised alternating movement (68 s) and rest (20 s) epochs to
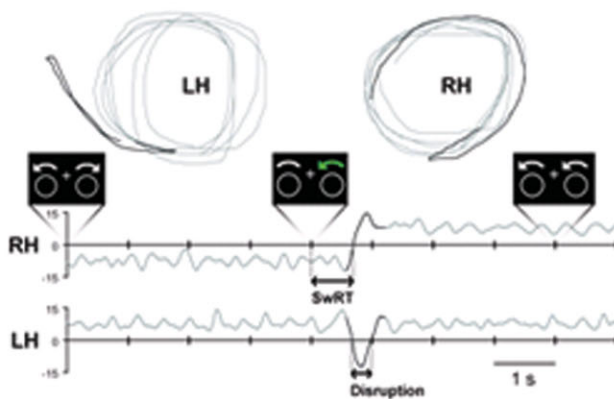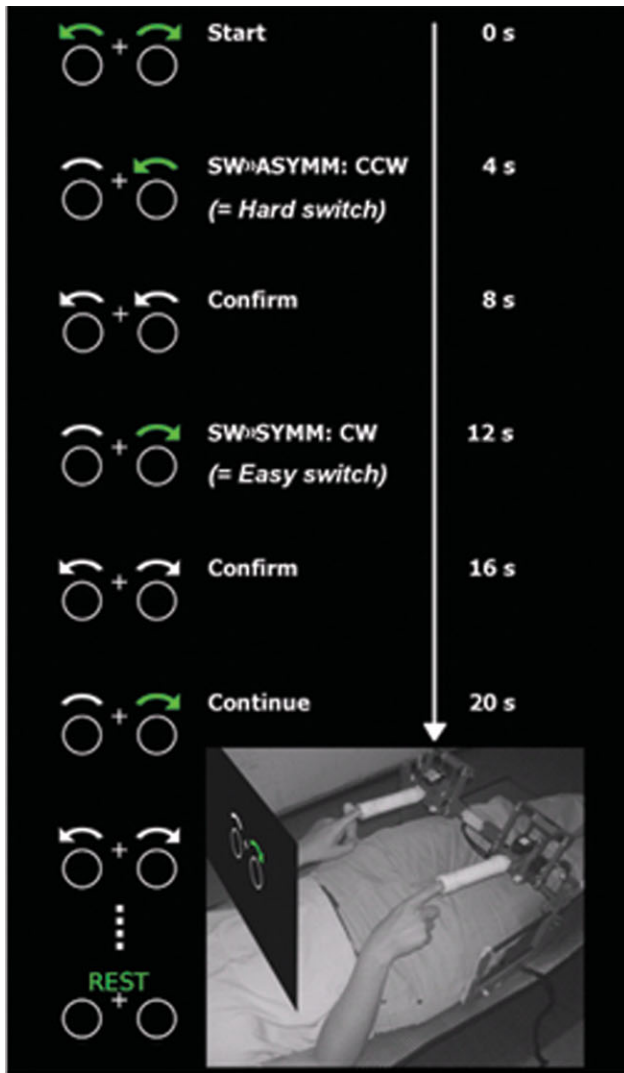
Figure 1.
Task performance in the MRI scanner. (**A**) Subject position and custom MRI compatible joysticks are shown. Visual stimuli were projected onto a screen that occluded vision below the shoulders and were viewed via a 45° mirror. Two circles and a central fixation cross were always visible. Imperative (green arrows) and confirmation cues (white arrows) were presented for 800 ms, separated by 4 s. Switching from symmetric to asymmetric (SW»ASYMM) or from asymmetric to symmetric (SW»SYMM) movement patterns required the right hand to change circling direction: Clockwise (CW) or counter-clockwise (CCW). (**B**) Representative trace from one participant performing symmetric circles followed by a switch to asymmetric circles (LH: left hand and RH: right hand). Top: Left- and right-hand joystick displacement, bottom: Radial velocity plotted against time (positive radial velocity = CW circles, negative radial velocity = CCW circles). The trace segments in dark gray highlight the right-hand switch and contralateral disruption of the left hand. [Color figure can be viewed in the online issue, which is available at wileyonlinelibrary.com.]

avoid fatigue. There were 14 Switch trials, 14 Continue trials, 4 Reverse trials, and 32 Confirmation trials per run. Reverse trials were signaled by two green arrows, cueing a switch of both hands. They were included to change left hand direction within a movement epoch, but were of no interest for the analysis. One of the four possible movement patterns was used as an initial pattern for each movement epoch and the order was counterbalanced across runs. In total, there were 70 Switch trials of the right hand (35 SW»SYMM, 35 SW»ASYMM) and 70 Continue trials. An algorithm was used to create pseudo randomized event sequences [Wager and Nichols, 2003], optimizing design efficiency for the contrast Switch > Continue while maintaining the unpredictability of the task. The hemodynamic response was effectively sampled every second, as event occurrence (multiples of 4 s) varied with respect to functional image acquisitions (every 3 s).

During both practice and scanning, joystick movements were registered by two fMRI compatible optical encoders (Hewlett-Packard, Malaysia; spatial resolution 0.18°) mounted along orthogonal axes. Custom LabVIEW software recorded the two-dimensional kinematics of each joystick (sample rate 100 Hz) and generated the visual display. Cues were projected onto a screen and viewed via a 45° mirror, attached to the head coil. Participants could see the visual display but the joysticks were obscured.

Image acquisition

A Siemens 3 T Magnetom Trio MRI scanner (Siemens, Erlangen, Germany) with an eight-channel head coil was used for image acquisition. For all subjects, a high-resolution T1-weighted structural image was acquired using magnetization prepared rapid gradient echo (MPRAGE; TR = 2,300 ms, echo time (TE) = 2.98 ms, $1.1 \times 1 \times 1$ mm voxels, field of view (FOV): 240×256, 160 sagittal slices). Functional data (fMRI) were acquired with a descending gradient echo planar imaging (EPI) pulse sequence for T2*-weighted images (TR = 3,000 ms, TE = 30 ms, flip angle = 90°, 50 oblique axial slices each 2.8 mm thick, interslice gap 0.28 mm, in-plane resolution 2.5×2.5 mm, 80×80 matrix). The diffusion tensor images were acquired using a single shot spin-echo (TR = 7,200 ms, TE = 81 ms, 56 sagittal slices of thickness 2.2 mm with 0.66 mm gap, in plane resolution 2.19×2.19 mm matrix 96×96). Diffusion sensitizing gradients were applied at a b-value of 1,000 s/mm^2, along a 64 noncollinear directions. In addition, one image with no diffusion weighting (b0) was acquired.

Data Analysis

Kinematic analysis

MATLAB 7.7 (Mathworks, Sherborn, MA) was used to analyze kinematic data. For each hand, a continuous estimate of angular velocity was determined by $\omega = d\theta/dt$

with $\theta = \arctan(x/y)$, where x and y describe the mean corrected values for vertical and horizontal joystick displacements, respectively. A second-order Butterworth low-pass filter (cutoff 5 Hz) was applied to ω. For trials where the right hand changed direction, switch response time (SwRT) was determined as the interval between stimulus onset and the first zero crossing of ω, indicating that cycling direction had reversed (Fig. 1B). The right-hand SwRT difference was also calculated for each individual by subtracting SwRT for SW»ASYMM from SW»SYMM (differential switch cost). Additionally, contralateral disruptions were recorded when left-hand direction was involuntarily reversed during the right-hand switch. Contralateral disruptions were divided into two types: (1) A partial contralateral disruption was classified when left-hand circling velocity ceased ($\omega = 0$ for at least 200 ms) or transiently reversed (e.g., $+\omega$ to $-\omega$ for at least 100 ms), followed by the resumption of correct left hand circling. (2) When left-hand direction reversed until the correct pattern was displayed, the trial was labeled as a complete contralateral disruption. A trial was classified as an error when (1) no right-hand switch occurred or (2) the right-hand SwRT was too fast (< 200 ms) or too slow (>2,000 ms). On average, this was <2% [range 0–17.6%; SD 3.1] of all trials for the TBI group. SwRT, variability of SwRT, percentage of partial and complete contralateral disruptions, and the duration of partial disruptions, were subjected to analysis of variance (ANOVA), with between-subjects factor Group (TBI, Young) and within-subject factors Resultant Pattern (SW»SYMM and SW»ASYMM) and Switch Direction of the right hand (CW, CCW). All statistical analyses were calculated with Statistica 8 (StatSoft, Tulsa, OK) using α-level of 0.05. Reported post hoc comparisons survived Bonferroni correction (effective α-level 0.0125).

Functional magnetic resonance analysis

Functional imaging data was preprocessed and analyzed with SPM5 (Wellcome Department of Imaging Neuroscience, University College, London) implemented in MATLAB 7.7 (Mathworks, Sherborn, MA).

Structural images were spatially normalized into standard Montreal Neurological Institute (MNI) space using a unified segmentation algorithm, which is less prone to normalization artifacts induced by changes in tissue signal [Ashburner and Friston, 2005; Crinion et al., 2007]. The unified segmentation algorithm is a generative model that combines tissue segmentation, bias correction and spatial normalization in the inversion of a single unified model [Ashburner and Friston, 2005]. To further refine the unified segmentation procedure for patients with clearly visible focal lesions ($N = 9$), a lesion mask was manually drawn in MRIcron (Chris Rorden, University of South Carolina), smoothed with a Gaussian kernel of 6 mm full width at half maximum (FWHM) and used as a cost function mask (for a visualization of focal lesion overlap see

Figure 1 Supporting Information). The registration process simply ignores the information within the mask and prevents contribution of lesion voxels to the normalization. This combination of the unified segmentation procedure and cost function masking outperforms cost function masking alone [Crinion et al., 2007].

The first three functional images of each subject's data set were discarded to allow for T1 equilibration. The remaining images were spatially realigned to the first image in the time series, then corrected for differences in slice acquisition time by temporal interpolation to the middle slice (reference slice = 25). Functional images were spatially coregistered to the anatomical image, and were normalized using the same transformation matrix applied to the anatomical image. Finally, the normalized functional images were smoothed with an isotropic 10 mm FWHM Gaussian kernel.

The preprocessed fMRI data were analyzed on a subject-by-subject basis using an event-related approach in the context of the General Linear Model [Friston et al., 1995]. Events were specified at the time of cue onset and modeled as delta functions convolved with the canonical hemodynamic response function (HRF) and its temporal derivative. Five conditions were specified: correct SW»A-SYMM trials, correct SW»SYMM trials, correct Continue trials, Confirmation, and Rest. Switch conditions were parametrically modulated by response time. An additional regressor modeled events of no interest such as Initiation trials, Reversals, Switch trials with complete contralateral disruptions, and their subsequent correction on Confirmation trials. In addition, realignment parameters were included as covariates of no interest to correct for confounding effects of head movement. Translational motions did not exceed 1 voxel (TBI: mean 0.55 mm, range 0.04–2.49 mm; Controls: mean 0.42 mm, range 0.06–2.12 mm). Rotations were on average 0.55 rad and ranged between 0.08 and 2.4 rad for the TBI group; in the control group rotations were on average 0.36 rad, ranging between 0.08 and 1.67 rad. The intensity changes attributable to global signal noise due to changes in the magnetic field over time were accounted for by using the time series of the mean signal from the white matter, cerebral spinal fluid, and out of brain voxels [Verhagen et al., 2006]. Data were filtered in the temporal domain using a high-pass cutoff of 1/128 Hz, and global differences in blood oxygen level-dependent signal were removed by scaling to the grand mean. For each subject, the contrast of Switch > Continue was created (by applying weights to the canonical HRF for each condition). Both Switch and Continue conditions consisted of identical visual cues, but only the Switch trials required a change of movement plan. Further, we created a contrast for Continue trials only, to check that the groups did not differ for this baseline condition. These contrast images were used as input for random effects (RFX) analysis of the two groups.

The principal question was whether TBI patients show increased cortical task related activity. Given the role of the BG in switching, we were also interested in whether TBI patients recruit these nuclei in a similar manner as healthy controls. We defined two second-level models to address this question. First, we were interested in regions with increased activity as a function of task across both groups. We used conjunction/disjunction analyses to isolate regions with common (Switch>Continue$_{TBI}$ ∩ Switch-Continue$_{CONTROLS}$) and unique (Switch>Continue$_{TBI}$ ⌐ Switch>Continue$_{CONTROLS}$ and Switch>Continue$_{CONTROLS}$ ⌐ Switch>Continue$_{TBI}$) activation [Nichols et al., 2005]. Second, we were interested in those regions that significantly increased or decreased their activity as a function of task in the TBI group, relative to the control group [(Switch > Continue$_{TBI}$) > (Switch > Continue$_{CONTROLS}$), (Switch > Continue$_{TBI}$) < (Switch > Continue$_{CONTROLS}$)]). For this analysis, a priori ROIs were defined based on previous studies on motor task switching and compensatory changes in TBI (see Introduction). The AAL template [Tzourio-Mazoyer et al., 2002] was used to construct anatomical ROIs for BG (caudate nucleus, putamen, and globus pallidus of each hemisphere), supplementary motor complex (preSMA and SMA-proper), ACC, and DLPFC. For the IFC (BA44; BA45) we made use of the Jülich histological atlas [Amunts et al., 1999]. As the subthalamic nucleus region (STN) is not included in the AAL template, it was defined as a $10 \times 10 \times 10$ cube centered at coordinate $x, y, z = \pm 10, -15, -5$ [Aron and Poldrack, 2006; Li et al., 2008]. Note that STN is a small structure and the resolution of whole brain fMRI is limited. We use the term to refer to STN and surrounding structures that may also fall within the boundary of the ROI. As an additional question we were interested in those regions that significantly increased their activity as a function of difficulty (SW»A-SYMM>Continue) > (SW»SYMM>Continue).

Whole brain statistical inference was performed at the cluster level (cluster defining height threshold $P < 0.001$), correcting for multiple comparisons over the search volume using family wise error correction (FWE) at $P < 0.05$. For the ROI analyses, statistical inference was performed at the voxel level, with FWE correction for multiple comparisons ($P < 0.05$).

The mean time course of all voxels in the significantly activated clusters and ROIs were extracted by means of the marsbar toolbox [Brett et al., 2002]. Unsmoothed images were used to avoid including signal from neighboring regions. Percent signal change (PSC) for Switch > Continue was determined from the parameter estimates to investigate inter-regional coupling, and relationships with behavior (SwRT, SwRT variability, and the percentage of complete left hand disruptions).

Diffusion tensor imaging (DTI) analysis

Diffusion data were preprocessed and analyzed using tools from the Oxford University Centre for Functional MRI of the Brain (FMRIB) software library (FSL Version 4.1). First, the b0 image of each subject was skull-stripped
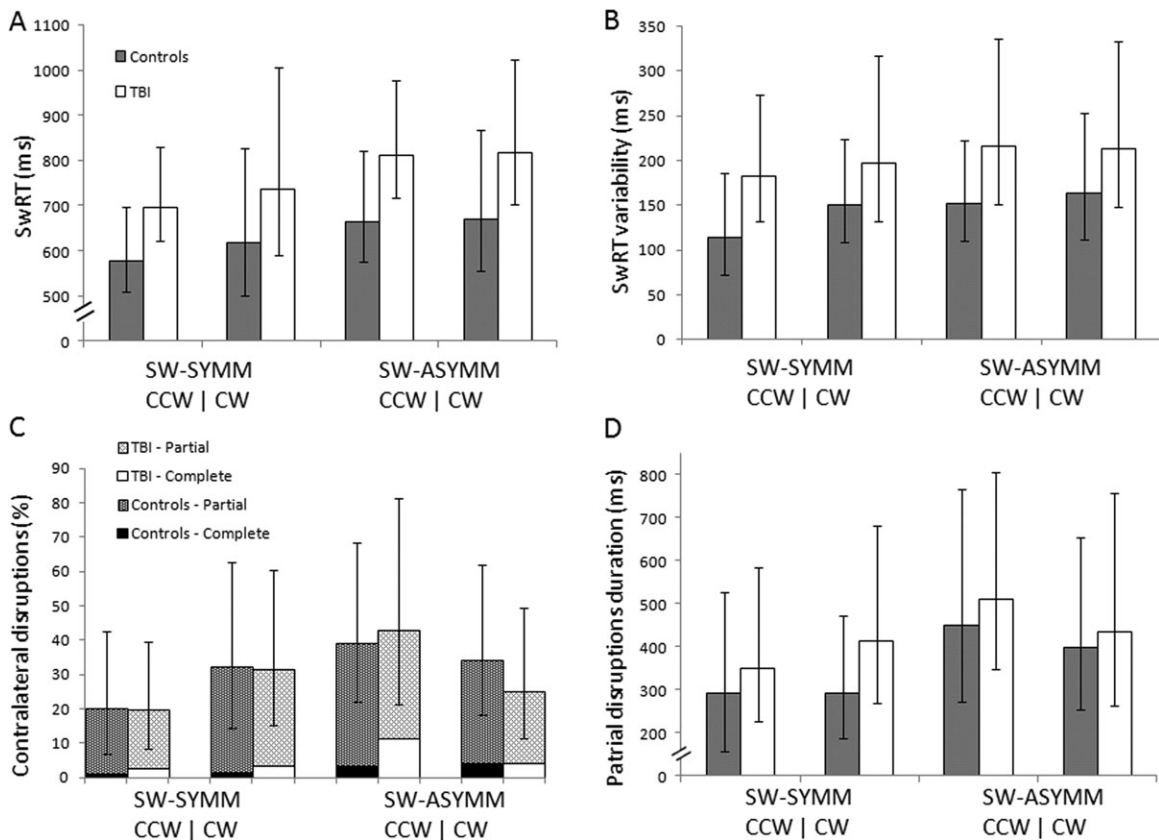
Figure 2.

Behavioral results. Top left: SwRT of the right hand. Top right: SwRT variability. Bottom left: Disruptions of contralateral (left) hand during right hand switches. Bottom right: Duration of partial contralateral disruptions. The combination of the pattern (SW»SYMM; SW»ASYMM) and switch direction (CW; CCW) determined the resulting movement pattern after the right hand switch. Results are reported as mean and 95% confidence interval of the population.

using the brain extraction tool [Smith, 2002]. The data was corrected for subject motion and eddy-current induced geometrical distortions, and the diffusion sensitizing gradients ("bvecs") were rotated to correct for motion. Using FDT, the diffusion tensor model was fit to the data, from which FA images were calculated.

For tract-based spatial statistics (TBSS) [Smith et al., 2006] all subjects' FA data was registered to a common space (the FA158 MNI space template) using a combination of affine and non-linear registration. A mean FA image was created, eroded to a skeleton and threshold at FA > 0.25. Each subject's aligned FA data were then projected onto this skeleton and the resulting alignment-invariant representation of the central trajectory of white matter pathways was used for voxelwise statistical analysis (Randomize, 10,000 permutations). The contrast TBI < Controls was examined using threshold free cluster enhancement (TFCE) [Smith and Nichols, 2009], with correction for multiple comparisons at α < 0.05.

To specifically look at the tracts between IFC, preSMA, and STN we applied a probabilistic diffusion model (BEDPOSTX) in subject diffusion space to calculate probability distributions on fiber direction at each voxel, allowing for estimates of more than one fiber direction within a voxel [Behrens et al., 2003, 2007]. The following tracts were delineated: (a) r-IFC to r-preSMA, (b) r-IFC to r-STN, (c) r-preSMA to r-STN, (d) l-preSMA to l-STN (e) l-IFC to l-preSMA, and (f) l-IFC to l-STN. A mask was used to prevent tracts crossing the midline. The seed masks were determined in MNI space (see Functional magnetic resonance analysis) and transformed to subject diffusion space using the inverse of the registrations generated during TBSS. Starting from each voxel in the seed region, 10,000 samples were generated with a curvature threshold of 0.2 and the samples reaching the target mask were retained. To determine the probable spatial trajectory of each tract, the maps representing the distribution of trajectories from seed to target were thresholded at a low level to remove noise
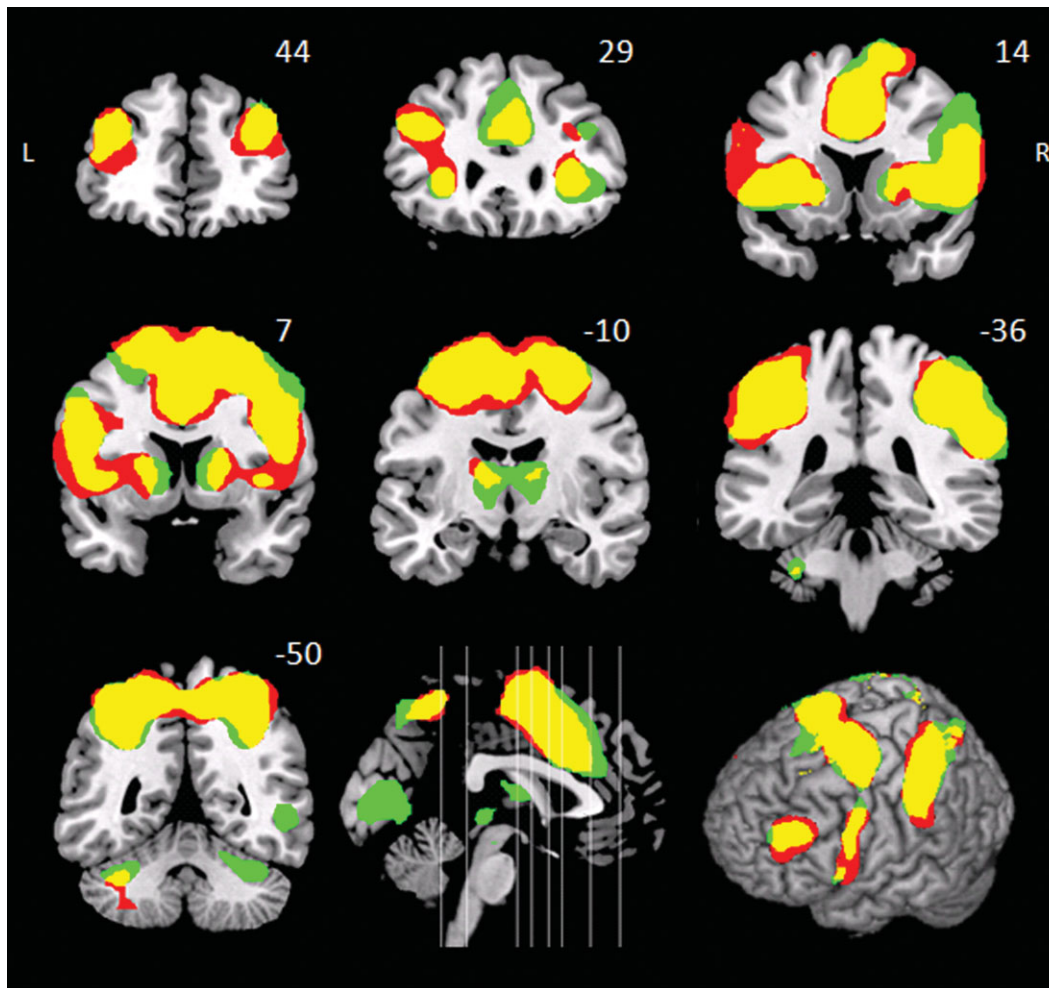
Figure 3.

Event-related analysis of Switch > Continue. Coronal sections. Yellow: Conjunction TBI ∩ Controls. Red: distinct activation in TBI. Green: distinct activation in the controls. Activations survived correction for multiple comparisons (RFX analysis, cluster level corrected at FWE $P < 0.05$). [Color figure can be viewed in the online issue, which is available at wileyonlinelibrary.com.]

(this was 0.02% of the maximum value in the connectivity map) [Aron et al., 2007], transformed to MNI space (using the TBSS registrations), binarized, and summed across participants. Voxels that were present in >95% of participants' maps were retained (Figure 6A, 3D render). The resulting MNI space tracts were used to extract the mean FA from each subjects' skeleton image generated during the TBSS analysis. Thus, the value for each tract can be thought to reflect the integrity of white matter projections to/from the nodes. Mean FA was correlated (a) with behavior (SwRT, SwRT variability, and percentage complete left hand disruptions) and (b) with percent signal change derived from l-preSMA, l-IFC, and STN clusters, to test the linkage between structure and function (Table III, Supporting Information Table III).

RESULTS

Behavioral Results

Overall (switch and continue trials) TBI patients were performing the correct pattern at confirmation 93.4% (SD 4.6) of the time. This indicates that they had no problems understanding the requirements of the task, and adhered to the visual cues.

SwRTs were significantly longer for the TBI group than for controls (GROUP: $F_{(1,47)} = 17.82$; $P < 0.001$; Fig. 2A). This effect is unlikely to be due to differences in circling frequency, as throughout the experiment, subjects were paced by a metronome at 50% of their maximal stable frequency. This frequency did not differ between groups [Controls 1.16 Hz (SD 0.12), TBI 1.15 Hz (SD 0.11), two-

sample t-test, and $P = 0.78$]. In accordance with the literature, switches to a symmetric pattern were initiated faster than switches to an asymmetric pattern for both groups (PATTERN: $F_{(1,47)} = 87.68$, $P < 0.001$; PATTERN * GROUP: $F_{(1,47)} = 2.25$, $P = 0.140$), and this was irrespective of whether the switch was executed in a clockwise or counter-clockwise direction (DIRECTION: $F_{(1,47)} = 2.40$, $P = 0.128$). TBI patients' switching performance was more variable than controls (GROUP: $F_{(1,47)} = 15.54$, $P < 0.001$). SwRT variability also increased in the SW»ASYMM condition as compared to SW»SYMM (PATTERN: $F_{(1,47)} = 15.20$; $P < 0.001$), but this effect was similar for the two groups (PATTERN * GROUP: $F_{(1,47)} = 0.00$; $P = 0.984$; Fig. 2B).

Partial left hand disruptions were more prevalent and lasted longer while switching to an asymmetric pattern than to a symmetric pattern (% partial CLD; PATTERN: $F_{(1,47)} = 13.56$; $P = 0.001$; duration partial CLD; PATTERN: $F_{(1,47)} = 12.990$; $P = 0.001$). These pattern effects did not differ significantly between the two groups (% partial CLD; PATTERN*GROUP: $F_{(1,47)} = 1.86$; $P = 0.179$; duration partial CLD; PATTERN*GROUP: $F_{(1,47)} = 0.25$; $P = 0.662$; Fig. 2C,D). Also, complete contralateral disruptions were more prevalent in the SW»ASYMM trials (PATTERN: $F_{(1,47)} = 17.02$; $P < 0.001$). Notably, the prevalence of complete left hand disruptions was higher for TBI patients (GROUP: $F_{(1,47)} = 8.820$; $P = 0.005$), especially for the switches to an asymmetric pattern in CCW direction (GROUP*PATTERN*DIRECTION: $F_{(1,47)} = 7.54$; $P = 0.009$; Bonferroni corrected post hoc t-test SW»ASYMM CCW: $P < 0.001$, all others n.s.; Fig. 2C).

fMRI Results

Motor switching network

Both groups activated a similar network during right hand switching, including bilateral insular cortex, IFC, DLPFC, dorsal, and ventral premotor cortex (PMd and PMv), putamen, superior and inferior parietal lobes, and cerebellum (lobule VI). Within the medial wall there was activation of ACC (both anterior and posterior rostral cingulate zones; RCZa, RCZp), preSMA and precuneus (Fig. 3, for nomenclature and stereotactic coordinates see Table II Supporting Information). The results of this conjunction analysis are very similar to the activation pattern shown previously in young and elderly subjects performing this task [Coxon et al., 2010] and comprise the core regions implicated in switching between task sets [Dosenbach et al., 2006].

Effect of coordination pattern

When contrasting the SW»SYMM and SW»ASYMM patterns, the more difficult SW»ASYMM pattern showed significantly higher activation in SMA-proper, bilateral putamen, right caudate, and left superior parietal lobule (SPL, BA7P; Table II, Supporting Information Fig. 2). This effect of pattern did not differ between TBI and controls.

TABLE II. Stereotactic coordinates of the local maxima showing differential cerebral activity during motor switching between TBI patients and healthy controls

Contrast	Search volume	Anatomical label	Functional label	Hemisphere	t-value	P-value	x	y	z
(Switch > Continue_TBI) > (Switch > Continue_CONTROLS)	ROI	Superior frontal gyrus: PreSMA	BA 6	L	4.11	0.011	-8	8	48
		Inferior frontal cortex	BA44	L	3.78	0.004	-60	10	13
(Switch > Continue_CONTROLS) > (Switch > Continue_TBI)	ROI	STN region		R	3.00	0.028	8	-10	-8
				L	2.90	0.020	-5	-10	-8
(SW»ASYMM > Continue) > (SW»SYMM > Continue)	Whole-brain	Superior frontal gyrus: SMA-proper	BA 6	R	8.76	<0.001	8	-18	65
				L	8.27		-15	-25	68
				L	7.67		-5	-20	63
		Putamen		R	7.86	<0.001	23	8	5
				L	6.44		-18	13	0
		Caudate		R	7.79	<0.001	15	-3	20
		Superior Parietal Lobule	BA 7P	L	3.87	0.001	-40	-60	48
				L	3.82		-25	-80	58
				L	3.66		-13	-88	43

Results of whole-brain analysis are corrected for multiple comparisons for search over the whole brain using cluster-level family wise inference ($P < 0.05$).
Results of ROI analysis are corrected for multiple comparisons over the ROI volume using voxel-level family wise inference (p<0.05).
Stereotactic coordinates are reported in Montreal Neurological Institute (MNI) space. Details on the anatomical and functional labeling can be found in the Methods and Results.
R, right; L, left; BA, Brodmann area; SMA, supplementary motor area, STN, subthalamic nucleus.
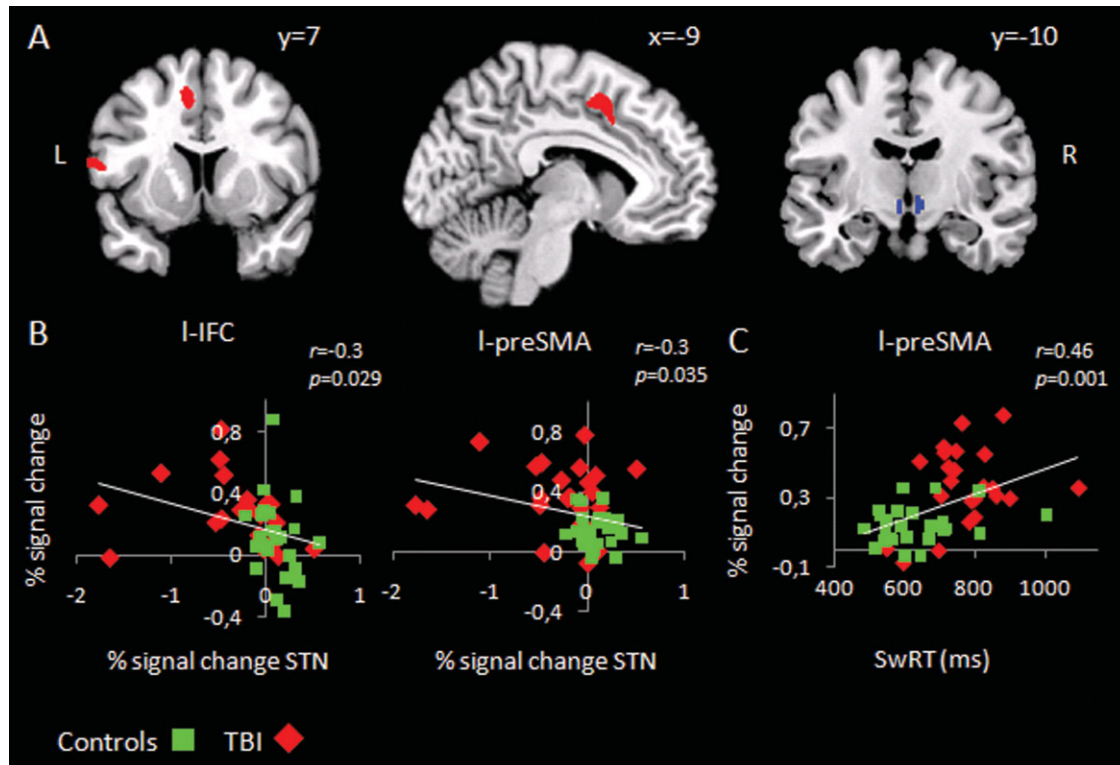
Figure 4.

Statistical parametric maps showing regions with differential switch related activity between TBI patients and controls. On the left, increased activity in left IFC and preSMA in TBI, superimposed on a coronal (left) and a sagittal (middle) slice. On the right, decreased activity in STN in TBI, superimposed on a coronal slice. ROI analysis, voxel level corrected at FWE $P < 0.05$. (**B**) Pearson correlation (two-tailed) across all participants between percent signal change (PSC) in left IFC and STN, and left preSMA and STN. (**C**) Pearson correlation (two-tailed) across all participants between PSC in left preSMA and SwRT. [Color figure can be viewed in the online issue, which is available at wileyonlinelibrary.com.]

There were no regions where activation was significantly higher for the opposite contrast (SW»SYMM > SW»ASYMM).

Between group analysis of a priori regions of interest

We hypothesized that TBI patients would show compensatory activation in cortical regions that support motor switching in an attempt to overcome their behavioral decline. To test this hypothesis we performed an ROI analyses on a priori selected regions of the motor switching network.

Two significant clusters showed increased activity in patients compared to controls (Fig. 4A; Table II). One cluster was located within the supplementary motor complex (local maximum at [−8 8 48]). Further division into preSMA and SMA-proper, by a vertical line from the anterior commissure ($y = 0$) [Johansen-Berg et al., 2004; Picard and Strick, 1996], showed that this cluster was almost completely located in preSMA. The second cluster was located within the left IFC (BA44) (local maximum at [−60 10 13]).

In contrast, control subjects activated the STN region more during switching than TBI patients (local maxima at [−5 −10 −8; 8 −10 −8]; Fig. 4A; Table II). These coordinates fall within the anatomical bounds of STN [Prodoehl et al., 2008]. None of the other ROI's showed a similar pattern of relative decrease of switching related activity in the TBI group. Moreover, no areas were found that were more active during Continue than during Switch trials in both comparisons.

Posthoc analysis revealed that higher activity in preSMA and left IFC was associated with lower STN activity (Fig. 4B). These relationships are robust to outlier removal. Across all participants percent signal change in preSMA was positively correlated with SwRT ($r = 0.46$; $P = 0.001$) and SwRT variability ($r = 0.39$; $P = 0.005$), showing that individuals with higher preSMA activity performed worse (Fig. 4C). Furthermore, lower STN activity was associated with higher SwRT ($r = −0.28$; $P = 0.056$), higher SwRT variability ($r = −0.33$; $P = 0.020$), and a higher percentage of complete left hand disruptions ($r = −0.33$; $P = 0.019$).

DTI Results

The tract-based spatial statistics analyses revealed widespread decline in FA throughout the skeleton for the TBI
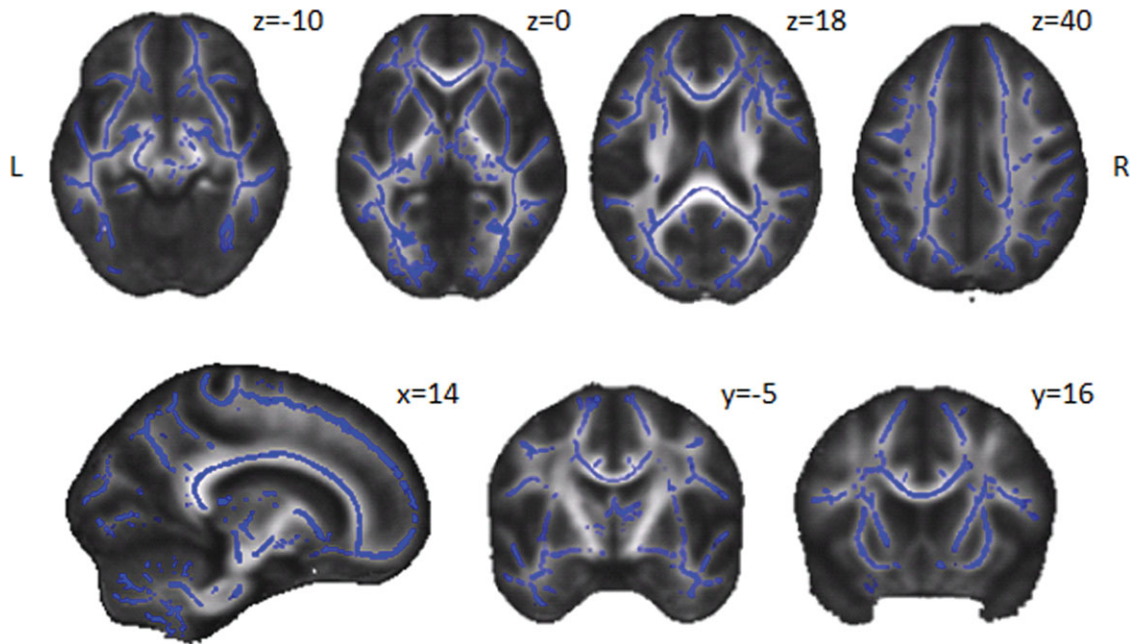
Figure 5.
Voxels with significantly reduced FA in the TBI group (TFCE correction) overlaid on mean FA image. [Color figure can be viewed in the online issue, which is available at wileyonlinelibrary.com.]

group (Fig. 5). The mean FA values derived from tracts between IFC, preSMA, and STN are reported in Table III. Mean FA was significantly reduced in the TBI group for all tracts except r-preSMA to r-STN.

In the next step, we correlated the mean FA values derived from the tracts with behavior. Across patients and controls, mean FA of the tract between l-IFC and l-preSMA predicted SwRTs (Fig. 6B). Subjects with lower struc-

tural integrity (FA) in the tract between l-IFC and l-preSMA showed worse performance. This pattern may be related to the association between function and behavior observed in preSMA (Table III).

As a final step, we tested whether there is a linkage between functional and structural individual differences. Therefore, we computed the correlation between percent signal change and FA. The results revealed a clear

TABLE III. Reduced structural connectivity and the relation with behavior

				SwRT			SwRT variability			% Complete left hand disruptions		
Tract	Mean (SD) TBI	Mean (SD) Controls	P-value	Overall	TBI	Controls	Overall	TBI	Controls	Overall	TBI	Controls
l-IFC to l-preSMA	0.44 (0.02)	0.48 (0.02)	<0.001	**−0.39**[a]	−0.06	**−0.24**	**−0.38**[b]	0.08	**−0.54**[a]	−0.33[b]	−0.09	−0.23
l-IFC to l-STN	0.51 (0.04)	0.53 (0.02)	0.004	−0.19	0.07	−0.11	−0.25	0.06	−0.44[b]	−0.26	−0.08	−0.25
l-preSMA to l-STN	0.54 (0.03)	0.57 (0.03)	0.004	−0.30[b]	−0.05	−0.20	−0.27	0.03	−0.37	−0.23	−0.02	−0.10
r-IFC to r-preSMA	0.47 (0.02)	0.50 (0.03)	<0.001	−0.34[b]	−0.07	−0.14	−0.29	0.16	−0.32	−0.29	0.07	−0.35
r-IFC to r-STN	0.51 (0.03)	0.54 (0.02)	<0.001	−0.26	0.04	−0.15	−0.24	0.15	−0.37	−0.27	0.01	−0.37
r-preSMA to r-STN	0.65 (0.04)	0.64 (0.04)	0.317	−0.19	0.09	−0.35	−0.11	−0.13	**−0.40**	0.03	−0.04	−0.11
Control variables												
TBSS skeleton	0.41 (0.02)	0.45 (0.02)	<0.001	−0.30[b]	−0.00	0.02	−0.31[b]	0.14	−0.34	−0.36[b]	−0.10	−0.32
Gender	8 F/15 M	15 F/11 M	0.11	−0.36[b]	−0.44[b]	−0.16	−0.31[b]	−0.43[b]	0.07	0.02	0.07	0.18

Mean FA from ROI's determined using probabilistic tractography. Group differences in FA were examined using one-tailed, two-sample t-tests. Group differences in gender were examined using a Chi squared test. The reported P-values are Bonferroni corrected for the number of comparisons ($\alpha = 0.00625$). One-tailed Pearson's correlation coefficients are reported for the relationship between FA and SwRT, SwRT variability and the percentage of complete left hand disruptions ([a]$P < 0.01$, [b]$P < 0.05$, bold front = significant after controlling for TBSS skeleton and gender).
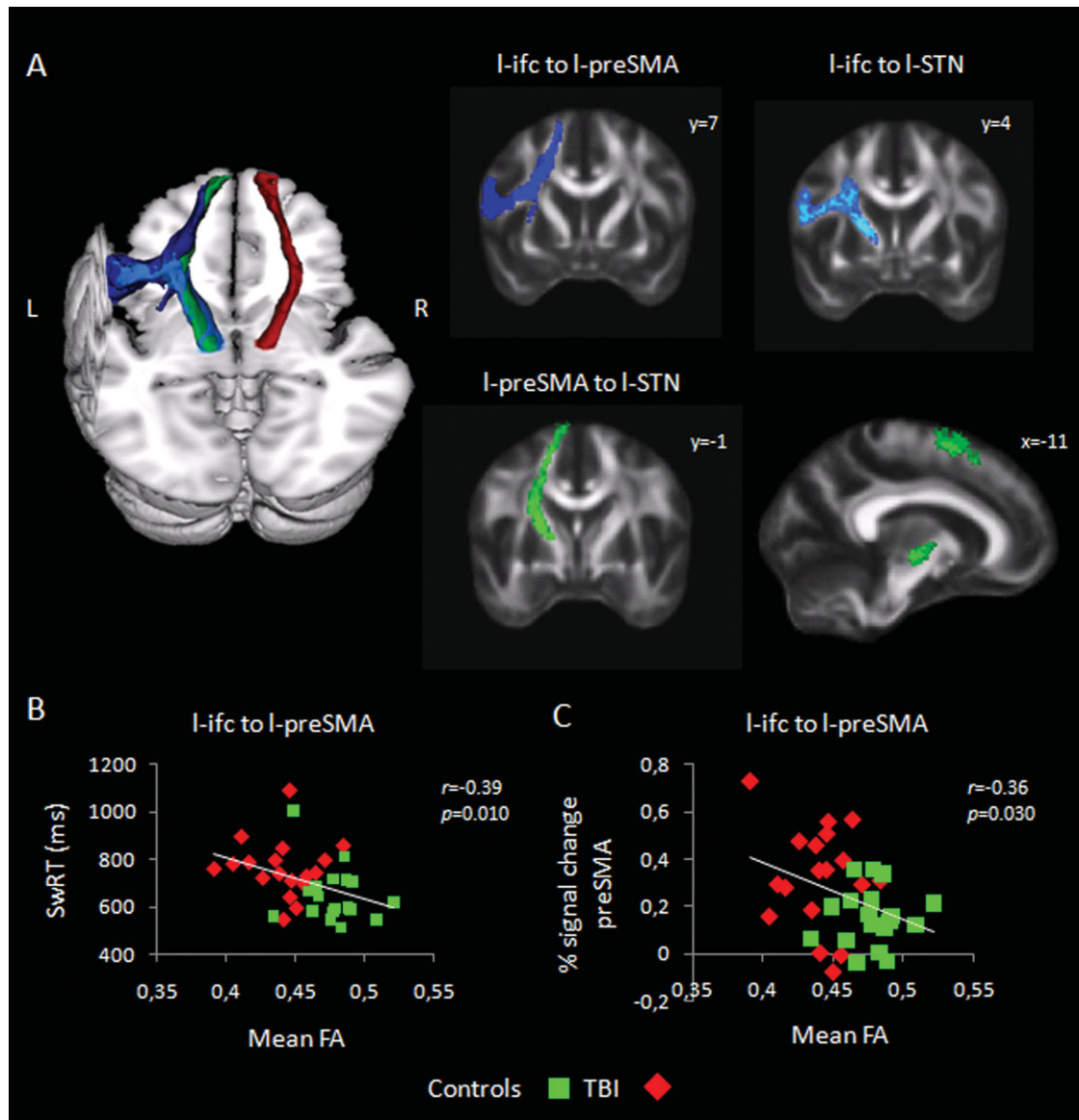
Figure 6.

(**A**) 3D render shows probabilistic tracts (> 95% of participants) from l-IFC to l-preSMA (blue), l-IFC to l-STN (light blue), l-pre-SMA to l-STN (green), and r-preSMA to r-STN (red). Coronal and sagittal sections further outline the trajectory of the individual tracts. (**B**) Pearson correlation (one-tailed) across all participants between mean FA values derived from l-IFC to l-preSMA tract and SwRT. (**C**) Pearson correlation (one-tailed) across all participants between mean FA values derived from l-IFC to l-preSMA tract and the percent signal change in left preSMA. [Color figure can be viewed in the online issue, which is available at wileyonlinelibrary.com.]

correlation between both measures (Supporting Information Table III; Fig. 6C). Lower FA in the tract from left IFC to left preSMA was associated with higher activity in preSMA ($r = -0.36$; $P < 0.05$) and lower STN activity ($r = 0.33$; $P < 0.05$). Moreover, subjects with higher preSMA activity during motor switching also showed lower FA in the tracts from left preSMA to left STN ($r = -0.40$; $P < 0.05$) and right IFC to right preSMA ($r = -0.45$; $P < 0.001$).

DISCUSSION

We used a bimanual coordination task to investigate the functional and structural underpinnings of motor switching in TBI. Relative to controls, patients overactivated preSMA and left IFC, and showed underactivation of the STN region. This altered brain activation pattern cannot be explained by mere motor output differences or deficits, as

bimanual circling frequency was equal in both groups. Moreover, deficits in white matter microstructure of the tracts connecting preSMA, IFC, and STN may mediate differences in functional activation pattern and underlie less proficient switching behavior. These results represent the first report of relationships between brain structure, function and behavior in the same group of moderate-severe TBI patients. In the following sections, we discuss the results and their relevance for current models of cognitive control in TBI.

Motor Task Switching Deficits in TBI Patients

The kinematic results showed that switching from a more stable symmetric coordination pattern to a less stable asymmetric pattern resulted in longer SwRT, more variable performance, and more contralateral disruptions. This general pattern of results has been reported previously in normal subjects [Byblow et al., 1999, 2000; Wenderoth et al., 2009]. Here, we extend these observations to TBI patients. Patients understood the requirements of this complex task and performed most aspects proficiently, initiating the right hand switch erroneously in only 2% of the trials. The direct nature of the cue, which explicitly indicated the direction of circling for the right hand, minimized the requirement to hold arbitrary stimulus-response mappings in working memory [Wenderoth et al., 2009]. However, TBI patients took longer to perform the switch, and were more variable in doing so. Moreover, they exhibited more involuntary reversals of left hand circling direction (complete contralateral disruptions). These performance deficits indicate that TBI patients are impaired in cognitively controlling their actions.

General Network Supporting Motor Task Switching

Activity common to both TBI patients and matched controls was observed in many cortical and subcortical regions seen in previous studies of task switching, including bilateral insular cortex, IFC, DLPFC, mesial frontal cortex, premotor areas, cerebellum, and putamen [Coxon et al., 2010; Derrfuss et al., 2005; Dosenbach et al., 2006]. Despite diffuse axonal injuries throughout the brain, TBI patients do activate the same general task-related network as their peers.

Pattern effect: Switching to symmetric or asymmetric coordination patterns

Both groups showed increased activation of SMA-proper and bilateral striatum (predominantly putamen) while switching to the more difficult asymmetric pattern. SMA-proper has been proposed to play a role in bimanual coordination, initiating the simultaneous actions of the two effectors and controlling their execution [Picton et al.,

2007; Swinnen and Wenderoth, 2004]. Recently, De Luca et al. [2010] showed that putamen activity is highly sensitive to pattern stability. Similar to our results bilateral putamen was more active when subjects were required to make an intentional switch to a more difficult, that is, less stable asymmetric pattern. We consider this increased putamen activity to support initiation of the new pattern, probably via the "direct" BG-cortex pathway, which is important for movement selection and initiation [Hikosaka and Isoda, 2010]. We found no evidence of a group by condition interaction, suggesting that TBI patients show a normal pattern of activity when initiating more difficult movement plans. This suggests that their slower and more variable switching behavior is unlikely to be explained by dysfunctional movement initiation circuitry.

Brain Activation Differences Between TBI Patients and Controls

Across both switching patterns, TBI patients were found to exhibit higher activation in preSMA and left IFC, and a relative decrease of activity in the STN region, suggesting that switching impairment in TBI patients is associated with distinct alterations in functional activity. The observed group differences in brain activation cannot be attributed to mere motor output differences, because overall task parameters known to modulate brain activation, such as bimanual circling frequency [Blinkenberg et al., 1996; Debaere et al., 2004], were well matched between the TBI patients and controls.

Cortical overactivation in TBI patients

Studies of cognitive control in moderate to severe TBI patients typically report more diffuse patterns of cortical recruitment or overactivation of prefrontal areas [Christodoulou et al., 2001; Kim et al., 2009; Newsome et al., 2008; Rasmussen et al., 2008; Scheibel et al., 2007]. For example, TBI patients show increased prefrontal activation during a working memory task when performance is equivalent to controls [Maruishi et al., 2007; Turner and Levine, 2008]. Investigations of Stroop task performance suggest increased prefrontal (DLPFC, ACC) and parietal activation in TBI during interference resolution due to the presence of irrelevant information [Mani et al., 2007; Soeda et al., 2005; Tlustos et al., 2011]. However, generalization of the latter results is limited due to the use of small samples (N = 5–11) and block designs which are more sensitive to sustained than trial-evoked activation. Moreover, we propose that Stroop performance relates to the ability to suppress irrelevant perceptual information, as opposed to motor switching processes. Here, we show increased activation in preSMA and left posterior IFC time-locked to the occurrence of successful motor task switching.

Switching between responses requires both inhibition of a primed action and facilitation of an alternative action. In

support of this assertion, Kenner et al. [2010] show that response inhibition and switching recruit similar networks, including the right IFC and preSMA. Right IFC has a role in the attentional capture of salient stimuli [Sharp et al., 2010] and is a critical node in the response inhibition network [Aron and Poldrack, 2006]. In our study, right IFC activation was common to both groups, whereas the TBI group overactivated left IFC compared to controls. This kind of hemispheric asymmetry reduction is often observed in elderly [Cabeza, 2002] and after stroke [Ward, 2004], and is usually considered compensatory. The additional left IFC recruitment in TBI patients could contribute to stimulus driven attention and inhibition of the ongoing movement.

TBI patients also showed a relative increase of activation in the preSMA. PreSMA is involved in situations where subjects have to stop an impending movement or when two procedures compete with each other [Aron and Poldrack, 2006; Coxon et al., 2010; Isoda and Hikosaka, 2007; Nachev et al., 2008; Rushworth et al., 2004], and damage to preSMA has been shown to impair these processes [Alexander et al., 2005; Clark et al., 2007; Picton et al., 2007; Rieger et al., 2003]. The preSMA exerts a strong influence on BG nuclei, with projections, not only to the striatum, but also to STN [Aravamuthan et al., 2007; Aron et al., 2007; Inase et al., 1999; Nambu et al., 2002]. These projections to STN, from preSMA, and/or IFC, may function to exert a "brake" on the BG motor loop [Aron, 2007; Hikosaka and Isoda, 2010]. We propose that the observed cortical overactivation reflects less efficient cortico-subthalamic interactions in TBI, as discussed next.

Subcortical underactivation in TBI patients

Alterations in BG activation during fMRI of cognitive tasks are scarcely reported in TBI. However, structural and pharmacological studies point to an involvement of subcortical nuclei in the deficits observed following TBI. A recent DTI study in mild to severe TBI patients [Little et al., 2010] has shown that disrupted integrity of connections between thalamus and cortex, due to diffuse axonal injuries, accounts for variance in executive function, attention, and memory domains. Furthermore, dopaminergic medication is beneficial for cognitive function in TBI [Bales et al., 2009; McAllister, 2006].

In this study, the TBI group showed significantly lower activation in the STN region. In contrast to the direct BG pathway, the indirect and hyperdirect BG pathways involve the STN and are thought to participate in the suppression of undesired actions [Mink, 1996; Nambu et al., 2002]. In rodents, lesions of the STN produce premature responses [Baunez et al., 2001], and in Parkinson's disease patients STN stimulation impairs responding in high conflict situations [Frank et al., 2007]. Recent fMRI studies show that preSMA, IFC, and STN are involved in conflict induced slowing and outright stopping [Aron and Poldrack, 2006; Aron et al., 2007; Coxon et al., 2009; Sharp

et al., 2010]. The recruitment of the hyperdirect pathway in switching might be important for breaking the response until response conflict is resolved. When several competing responses are activated, the STN receives excitatory input from the cortex and sends a strong global "nogo" signal allowing the BG to consider fully all possible options before selecting the appropriate action [Frank, 2006]. We propose that TBI patients attempt to activate the STN region via increased cortical activation in left IFC and preSMA; however, they seem less able to modulate the STN compared to controls. Computational simulations of the BG circuit have shown that cortical lesions can eliminate oscillations in the STN [Frank, 2006]. Therefore, we took a closer look at the anatomical connectivity between preSMA, IFC, and STN, and their relation to behavior and brain function.

Relationship Between Structure, Function, and Behavior

DTI provides information about anatomical connectivity in the brain by measuring the anisotropic diffusion of water in white matter tracts. The measure most commonly derived from diffusion data to index white matter integrity is FA, which quantifies how strongly directional the local tract structure is. Previous studies have shown that DTI is very sensitive in localizing white matter damage in TBI [Kennedy et al., 2009; Kinnunen et al., 2011; Kraus and McArthur, 1996; Niogi et al., 2008; Salmond et al., 2006; Sidaros et al., 2008]. A problem in multisubject diffusion imaging analyses is the registration to common space. The method of Smith et al. [2006] allows for a more sensitive and objective interpretation of the results. By making use of the FA skeleton instead of the whole brain, it is more robust to systematic group differences, such as brain atrophy. Here, we replicate the results from Kinnunen et al. [2011], showing a widespread reduction in FA throughout the whole white matter skeleton in TBI. This widespread reduction in white matter integrity is a direct consequence of the trauma, but can also be due to chronic inflammation processes after TBI [Ramlackhansingh et al., 2011]. For the rest of the analyses, we focused on the task-relevant tracts connecting preSMA, IFC, and STN.

Animal work has revealed that both preSMA and IFC have projections to the STN [Inase et al., 1999; Nambu et al., 2002], and diffusion weighted imaging tractography provides complementary evidence in humans [Aravamuthan et al., 2007; Aron et al., 2007]. We made use of a similar probabilistic tractography approach, to determine the most likely tract trajectory through MNI space. The results suggest that damage to these specific tracts can affect behavioral performance. Across patients and controls, subjects with lower FA in tracts connecting IFC and preSMA, and left preSMA with left STN, showed higher SwRTs, higher variability and more complete left hand disruptions. The results suggest that damage to the tracts

responsible for normal intra-individual differences in motor switching proficiency because of TBI, may shift the patients towards the lower end of the existing structure-function-behavior spectrum.

Next, we were interested in whether variations in BOLD would covary with structural connectivity of the tracts connecting preSMA, IFC, and the STN region. There is growing evidence for such a linkage between BOLD and white matter connectivity data. For instance, Forstmann et al. [2008] found a positive correlation between structural integrity of the anterior inferior fronto-occipital fasciculus and the BOLD covariation in the adjacent IFC. Here, subjects with lower FA in the tract connecting left preSMA with left IFC, showed higher preSMA activity and lower STN activity during switching. Based on the results, we speculate that TBI patients with the most severe damage to white matter tracts connecting preSMA, IFC, and STN, fail to modulate the STN via preSMA and/or IFC, resulting in less proficient switching behavior.

CONCLUSION

We investigated motor task switching in a large group of moderate to severe TBI patients. Our findings indicate that TBI patients show clear switching impairments, which directly relate to the activity in preSMA, left IFC, and STN, as well as the white matter microstructural properties of the tracts connecting these areas, which are thought to be important for successful inhibition of inappropriate actions, a constitute process of switching.

REFERENCES

Alexander MP, Stuss DT, Shallice T, Picton TW, Gillingham S (2005): Impaired concentration due to frontal lobe damage from two distinct lesion sites. Neurology 65:572–579

Amunts K, Schleicher A, Burgel U, Mohlberg H, Uylings HBM, Zilles K (1999): Broca's region revisited: Cytoarchitecture and intersubject variability. J Comp Neurol 412:319–341

Aravamuthan BR, Muthusamy KA, Stein JF, Aziz TZ, Johansen-Berg H (2007): Topography of cortical and subcortical connections of the human pedunculopontine and subthalamic nuclei. Neuroimage 37:694–705

Aron AR (2007): The neural basis of inhibition in cognitive control. Neuroscientist 13:214–228

Aron AR, Poldrack RA (2006): Cortical and subcortical contributions to stop signal response inhibition: Role of the subthalamic nucleus. J Neurosci 26:2424–2433

Aron AR, Behrens TE, Smith S, Frank MJ, Poldrack RA (2007): Triangulating a cognitive control network using diffusion-weighted magnetic resonance imaging (MRI) and functional MRI. J Neurosci 27:3743–3752

Ashburner J, Friston KJ (2005): Unified segmentation. Neuroimage 26:839–851

Bales JW, Wagner AK, Kline AE, Dixon CE (2009): Persistent cognitive dysfunction after traumatic brain injury: A dopamine hypothesis. Neurosci Biobehav Rev 33:981–1003

Baunez C, Humby T, Eagle DM, Ryan LJ, Dunnett SB, Robbins TW (2001): Effects of STN lesions on simple vs choice reaction time tasks in the rat: Preserved motor readiness, but impaired response selection. Eur J Neurosci 13:1609–1616

Blinkenberg M, Bonde C, Holm S, Svarer C, Andersen J, Paulson OB, Law I (1996): Rate dependence of regional cerebral activation during performance of a repetitive motor task: A PET study. J Cereb Blood Flow Metab 16:794–803

Brett M, Anton JL, Valabregue R, Poline JB (2002): Region of interest analysis using an SPM toolbox [abstract] Presented at the 8th International Conference on Functional Mapping of the Human Brain, June 2-6, 2002, Sendai, Japan. Available on CD-ROM in Neuroimage 16.

Bruns TJ, Hauser WA (2003): The epidemiology of traumatic brain injury: A review. Epilepsia 44:2–10.

Byblow WD, Chua R, Bysouth-Young DF, Summers JJ (1999): Stabilisation of bimanual coordination through visual coupling. Hum Mov Sci 18:281–305

Byblow WD, Lewis GN, Stinear JW, Austin NJ, Lynch M (2000): The subdominant hand increases the efficacy of voluntary alterations in bimanual coordination. Exp Brain Res 131:366–374.

Cabeza R (2002): Hemispheric asymmetry reduction in older adults: The HAROLD model. Psychol Aging 17:85–100.

Carson RG, Thomas J, Summers JJ, Walters MR, Semjen A (1997): The dynamics of bimanual circle drawing. QJEP Section A. Hum Exp Psychol 50:664–683.

Christodoulou C, DeLuca J, Ricker JH, Madigan NK, Bly BM, Lange G, Kalnin AJ, Liu WC, Steffener J, Diamond BJ, Ni AC (2001): Functional magnetic resonance imaging of working memory impairment after traumatic brain injury. J Neurol Neurosurg Psychiatry 71:161–168

Clark L, Blackwell AD, Aron AR, Turner DC, Dowson J, Robbins TW, Sahakian BJ (2007): Association between response inhibition and working memory in adult ADHD: A link to right frontal cortex pathology? Biol Psychiatry 61:1395–1401

Colantonio A, Ratcliff G, Chase S, Kelsey S, Escobar M, Vernich L (2004): Long-term outcomes after moderate to severe traumatic brain injury. Disabil Rehabil 26:253–261.

Coxon JP, Stinear CM, Byblow WD (2009): Stop and go: The neural basis of selective movement prevention. J Cogn Neurosci 21:1193–1203.

Coxon JP, Goble DJ, Van IA, De VJ, Wenderoth N, Swinnen SP (2010): Reduced Basal Ganglia Function When Elderly Switch between Coordinated Movement Patterns. Cereb Cortex 20:2368–79.

Crinion J, Ashbumer J, Leff A, Brett M, Price C, Friston K (2007): Spatial normalization of lesioned brains: Performance evaluation and impact on fMRI analyses. Neuroimage 37:866–875.

De Luca C, Jantzen KJ, Comani S, Bertollo M, Kelso JAS (2010): Striatal Activity during Intentional Switching Depends on Pattern Stability. J Neurosci 30:3167–3174.

Debaere F, Wenderoth N, Sunaert S, van Hecke P, Swinnen SP (2004): Cerebellar and premotor function in bimanual coordination: Parametric neural responses to spatiotemporal complexity and cycling frequency. Neuroimage 21:1416–1427.

Derrfuss J, Brass M, Neumann J, von Cramon DY (2005): Involvement of the inferior frontal junction in cognitive control: Meta-analyses of switching and stroop studies. Hum Brain Mapp 25:22–34.

Dosenbach NUF, Visscher KM, Palmer ED, Miezin FM, Wenger KK, Kang HSC, Burgund ED, Grimes AL, Schlaggar BL, Petersen SE (2006): A core system for the implementation of task sets. Neuron 50:799–812.

Draper K, Ponsford J (2008): Cognitive functioning ten years following traumatic brain injury and rehabilitation. Neuropsychol 22:618–625.

Forstmann BU, Jahfari S, Scholte HS, Wolfensteller U, van den Wildenberg WPM, Ridderinkhof KR (2008): Function and structure of the right inferior frontal cortex predict individual differences in response inhibition: A model-based approach. J Neurosci 28:9790–9796.

Frank MJ (2006): Hold your horses: A dynamic computational role for the subthalamic nucleus in decision making. Neural Netw 19:1120–1136.

Frank MJ, Scheres A, Sherman SJ (2007): Understanding decision-making deficits in neurological conditions: Insights from models of natural action selection. Philos Trans R Soc B Biol Sci 362:1641–1654.

Friston KJ, Holmes AP, Poline JB, Grasby PJ, Williams SCR, Frackowiak RSJ, Turner R (1995): Analysis of Fmri Time-Series Revisited. Neuroimage 2:45–53.

Gentry LR, Godersky JC, Thompson B (1988): Mr Imaging of Head Trauma-Review of the Distribution and Radiopathologic Features of Traumatic Lesions. Am J Roentgenol 150:663–672.

Hikosaka O, Isoda M (2010): Switching from automatic to controlled behavior: Cortico-basal ganglia mechanisms. Trends Cogn Sci 14:154–161.

Inase M, Tokuno H, Nambu A, Akazawa T, Takada M (1999): Corticostriatal and corticosubthalamic input zones from the presupplementary motor area in the macaque monkey: Comparison with the input zones from the supplementary motor area. Brain Res 833:191–201.

Isoda M, Hikosaka O (2007): Switching from automatic to controlled action by monkey medial frontal cortex. Nat Neurosci 10:240–248.

Johansen-Berg H, Behrens TEJ, Robson MD, Drobnjak I, Rushworth MFS, Brady JM, Smith SM, Higham DJ, Matthews PM (2004): Changes in connectivity profiles define functionally distinct regions in human medial frontal cortex. Proc Natl Acad Sci USA 101:13335–13340.

Kelso JAS, Fuchs A (1995): Self-Organizing Dynamics of the Human Brain-Critical Instabilities and Silnikov Chaos. Chaos 5:64–69.

Kennedy MRT, Wozniak JR, Muetzel RL, Mueller BA, Chiou HH, Pantekoek K, Lim KO (2009): White matter and neurocognitive changes in adults with chronic traumatic brain injury. J Int Neuropsychol Soc 15:130–136.

Kenner NM, Mumford JA, Hommer RE, Skup M, Leibenluft E, Poldrack RA (2010): Inhibitory Motor Control in Response Stopping and Response Switching. J Neurosci 30:8512–8518.

Kim YH, Yoo WK, Ko MH, Park CH, Kim ST, Na DL (2009): Plasticity of the Attentional Network After Brain Injury and Cognitive Rehabilitation. Neurorehabil Neural Repair 23:468–477.

Kinnunen KM, Greenwood R, Powell JH, Leech R, Hawkins PC, Bonnelle V, Patel MC, Counsell SJ, Sharp DJ (2011): White matter damage and cognitive impairment after traumatic brain injury. Brain 134:449–463.

Kraus JF, McArthur DL (1996): Epidemiologic aspects of brain injury. Neurol Clin 14:435–450.

Larson MJ, Perlstein WM, Demery JA, Stigge-Kaufman DA (2006): Cognitive control impairments in traumatic brain injury. J Clin Exp Neuropsychol 28:968–986.

Levin H, Kraus MF (1994): The frontal lobes and traumatic brain injury. J Neuropsychiatry Clin Neurosci 6:443–454.

Levin HS, Hanten G, Zhang LF, Swank PR, Hunter J (2004): Selective impairment of inhibition after TBI in children. J Clin Exp Neuropsychol 26:589–597.

Li CSR, Yan P, Sinha R, Lee TW (2008): Subcortical processes of motor response inhibition during a stop signal task. Neuroimage 41:1352–1363.

Little DM, Kraus MF, Joseph J, Geary EK, Susmaras T, Zhou XJ, Pliskin N, Gorelick PB (2010): Thalamic integrity underlies executive dysfunction in traumatic brain injury. Neurology 74:558–564.

Maas AIR, Stocchetti N, Bullock R (2008): Moderate and severe traumatic brain injury in adults. Lancet Neurol 7:728–741.

Malec JF, Brown AW, Leibson CL, Flaada JT, Mandrekar JN, Diehl NN, Perkins PK (2007): The Mayo classification system for traumatic brain injury severity. J Neurotrauma 24:1417–1424.

Mani TM, Miller LS, Yanasak N, Macciocchi S (2007): Variability in Stroop task performance and functional activation among a small brain-injured group. Neurocase 13:229–236.

Maruishi M, Miyatani M, Nakao T, Muranaka H (2007): Compensatory cortical activation during performance of an attention task by patients with diffuse axonal injury: A functional magnetic resonance imaging study. J Neurol Neurosurg Psychiatry 78:168–173.

McAllister TW (2006): Catecholaminergic modulation of memory after mild and moderate TBI: Evidence from MRI studies. Brain Cogn 60:189.

McDonald BC, Flashman LA, Saykin AJ (2002): Executive dysfunction following traumatic brain injury: Neural substrates and treatment strategies. Neurorehabilitation 17:333–344.

Mecklinger AD, von Cramon DY, Springer A, Matthes-von CG (1999): Executive control functions in task switching: Evidence from brain injured patients. J Clin Exp Neuropsychol 21:606–619.

Mink JW (1996): The basal ganglia: Focused selection and inhibition of competing motor programs. Prog Neurobiol 50:381–425.

Monsell S (2003): Task switching. Trends Cogn Sci 7:134–140.

Nachev P, Kennard C, Husain M (2008): Functional role of the supplementary and pre-supplementary motor areas. Nat Rev Neurosci 9:856–869.

Nambu A, Tokuno H, Takada M (2002): Functional significance of the cortico-subthalamo-pallidal 'hyperdirect' pathway. Neurosci Res 43:111–117.

Newsome MR, Steinberg JL, Scheibel RS, Troyanskaya M, Chu Z, Hanten G, Lu H, Lane S, Lin X, Hunter JV, Vasquez C, Zientz J, Li X, Wilde EA, Levin HS (2008): Effects of traumatic brain injury on working memory-related brain activation in adolescents. Neuropsychology 22:419–425.

Nichols T, Brett M, Andersson J, Wager T, Poline JB (2005): Valid conjunction inference with the minimum statistic. Neuroimage 25:653–660.

Niogi SN, Mukherjee P, Ghajar J, Johnson C, Kolster RA, Sarkar R, Lee H, Meeker M, Zimmerman RD, Manley GT, McCandliss BD (2008): Extent of microstructural white matter injury in postconcussive syndrome correlates with impaired cognitive reaction time: A 3T diffusion tensor imaging study of mild traumatic brain injury. Am J Neuroradiol 29:967–973.

Oldfield RC (1971): Assessment and Analysis of Handedness-Edinburgh Inventory. Neuropsychologia 9:97–113.

Perlstein WM, Larson MJ, Dotson VM, Kelly KG (2006): Temporal dissociation of components of cognitive control dysfunction in severe TBI: ERPs and the cued-Stroop task. Neuropsychologia 44:260–274.

Picard N, Strick PL (1996): Motor areas of the medial wall: A review of their location and functional activation. Cereb Cortex 6:342–353.

Picton TW, Stuss DT, Alexander MP, Shallice T, Binns MA, Gillingham S (2007): Effects of focal frontal lesions on response inhibition. Cereb Cortex 17:826–838.

Prodoehl J, Yu H, Little DM, Abraham I, Vaillancourt DE (2008): Region of interest template for the human basal ganglia: Comparing EPI and standardized space approaches. Neuroimage 39:956–965.

Ramlackhansingh AF, Brooks DJ, Greenwood RJ, Bose SK, Turkheimer FE, Kinnunen KM, Gentleman S, Heckemann RA, Gunanayagam K, Gelosa G, Sharp DJ (2011): Inflammation after trauma: Microglial activation and traumatic brain injury. Ann Neurol 70:374–383.

Rasmussen IA, Xu J, Antonsen IK, Brunner J, Skandsen T, Axelson DE, Berntsen EM, Lydersen S, Haberg A (2008): Simple Dual Tasking Recruits Prefrontal Cortices in Chronic Severe Traumatic Brain Injury Patients, But Not in Controls. J Neurotrauma 25:1057–107.

Rieger M, Gauggel S, Burmeister K (2003): Inhibition of ongoing responses following frontal, nonfrontal, and basal ganglia lesions. Neuropsychol 17:272–282.

Rushworth MFS, Walton ME, Kennerley SW, Bannerman DM (2004): Action sets and decisions in the medial frontal cortex. Trends Cogn Sci 8:410–417.

Salmond CH, Menon DK, Chatfield DA, Williams GB, Pena A, Sahakian BJ, Pickard JD (2006): Diffusion tensor imaging in chronic head injury survivors: Correlations with learning and memory indices. Neuroimage 29:117–124.

Scheibel RS, Newsome MR, Steinberg JL, Pearson DA, Rauch RA, Mao H, Troyanskaya M, Sharma RG, Levin HS (2007): Altered brain activation during cognitive control in patients with moderate to severe traumatic brain injury. Neurorehabil Neural Repair 21:36–45.

Scheid R, Walther K, Guthke T, Preul C, von Cramon DY (2006): Cognitive sequelae of diffuse axonal injury. Arch Neurol 63:418–424.

Seignourel PJ, Robins DL, Larson MJ, Demery JA, Cole M, Perlstein WM (2005): Cognitive control in closed head injury: Context maintenance dysfunction or prepotent response inhibition deficit? Neuropsychol 19:578–590.

Sharp DJ, Bonnelle V, De Boissezon X, Beckmann CF, James SG, Patel MC, Mehta MA (2010): Distinct frontal systems for response inhibition, attentional capture, and error processing. Proc Natl Acad Sci USA 107:6106–6111.

Sidaros A, Engberg A, Sidaros K, Liptrot MG, Herning M, Petersen P, Paulson OB, Jernigan TL, Rostrup E (2008): Diffusion tensor imaging during recovery from severe traumatic brain injury and relation to clinical outcome: A longitudinal study. Brain 131:559–572.

Smith SM (2002): Fast robust automated brain extraction. Hum Brain Mapp 17:143–155.

Smith SM, Jenkinson M, Johansen-Berg H, Rueckert D, Nichols TE, Mackay CE, Watkins KE, Ciccarelli O, Cader MZ, Matthews PM, Behrens TEJ (2006): Tract-based spatial statistics: Voxelwise analysis of multi-subject diffusion data. Neuroimage 31:1487–1505.

Soeda A, Nakashima T, Okumura A, Kuwata K, Shinoda J, Iwama T (2005): Cognitive impairment after traumatic brain injury: A functional magnetic resonance imaging study using the Stroop task. Neuroradiol 47:501–506.

Sosin DM, Sniezek JE, Thurman DJ (1996): Incidence of mild and moderate brain injury in the United States, 1991. Brain Inj 10:47–54.

Swinnen SP (2002): Intermanual coordination: From behavioural principles to neural-network interactions. Nat Rev Neurosci 3:350–361.

Swinnen SP, Wenderoth N (2004): Two hands, one brain: Cognitive neuroscience of bimanual skill. Trends Cogn Sci 8:18–25.

Tagliaferri F, Compagnone C, Korsic M, Servadei F, Kraus J (2006): A systematic review of brain injury epidemiology in Europe. Acta Neurochir 148:255–268.

Tlustos SJ, Chiu CYP, Walz NC, Holland SK, Bernard L, Wade SL (2011): Neural Correlates of Interference Control in Adolescents with Traumatic Brain Injury: Functional Magnetic Resonance Imaging Study of the Counting Stroop Task. J Int Neuropsychol Soc 17:181–189.

Turner GR, Levine B (2008): Augmented neural activity during executive control processing following diffuse axonal injury. Neurology 71:812–818.

Turner GR, McIntosh AR, Levine B (2011): Prefrontal Compensatory Engagement in TBI is due to Altered Functional Engagement Of Existing Networks and not Functional Reorganization. Front Syst Neurosci 5:9.

Tzourio-Mazoyer N, Landeau B, Papathanassiou D, Crivello F, Etard O, Delcroix N, Mazoyer B, Joliot M (2002): Automated anatomical labeling of activations in SPM using a macroscopic anatomical parcellation of the MNI MRI single-subject brain. Neuroimage 15:273–289.

Verhagen L, Grol MJ, Dijkerman HC, Toni I (2006): Studying visually-guided reach to grasp movements in an MR-environment. Neuroimage 31:S1 (Twelfth Annual Meeting of the Organization for Human Brain Mapping, Florence, Italy).

Wager TD, Nichols TE (2003): Optimization of experimental design in fMRI: A general framework using a genetic algorithm. Neuroimage 18:293–309.

Ward NS (2004): Functional reorganization of the cerebral motor system after stroke. Curr Opin Neurobiol 17:725–730.

Wenderoth N, Van Dooren M, Vandebroek A, De Vos J, Vangheluwe S, Stinear CM, Byblow WD, Swinnen SP (2009): Conceptual Binding: Integrated Visual Cues Reduce Processing Costs in Bimanual Movements. J Neurophysiol 102:302–311.